Ligand Effects in the Models and Mimics of Oxyhemocyanin and Oxytyrosinase. A Density Functional Study of Reversible Dioxygen Binding and Reversible O−O Bond Cleavage

Attila Bérces

Steacie Institute for Molecular Sciences, National Research Council Canada, 100 Sussex Drive, Ottawa, Ontario, K1A 0R6 Canada

Received April 3, 1997[⊗]

We studied the energetics of dioxygen binding and the core isomerization between the $Cu_2(\mu\text{-}\eta^2\text{:}\eta^2\text{-}O_2)$ and $Cu_2(\mu\text{-}O)_2$ core structures of $\{[LCu]_2O_2\}^{2+}$, L = 1,4,7-triazacyclononane (**1**) and L = hydrotris(pyrazolyl)borate (**2**), by gradient-corrected density functional methods. N-Substituted derivatives of **1** and **2** are synthetic inorganic mimics of oxyhemocyanin with similar physical and spectroscopic properties but different chemical behavior. The calculated dioxygen binding energies of **1** and **2** are −60 and −184 kJ/mol, respectively, in line with the observation that **1** binds oxygen reversibly and **2** does so irreversibly. Bond energy decomposition showed that orbital interactions contribute equally to the binding energy of **1** and **2**, which explains the similarities in their spectral properties. Electrostatic interactions due to the negatively charged ligand are responsible for stronger binding in **2**. The core isomerization energies for isomerization from the $Cu_2(\mu\text{-}\eta^2\text{:}\eta^2\text{-}O_2)$ to the $Cu_2(\mu\text{-}O)_2$ isomers of **1** and **2** are +1 and +12 kJ/mol, respectively. The barrier heights of the core isomerizations of **1** and **2** relative to the $Cu_2(\mu\text{-}\eta^2\text{:}\eta^2\text{-}O_2)$ isomer are 33 and 37 kJ/mol, respectively. The results on **1** are in line with the experimentally observed fast and reversible interconversion between the two isomers while these data on **2** suggest that the observation of **2** in the $(\mu\text{-}O)_2$ isomer was only prevented by its thermal instability. We also considered a purely theoretical model compound, $\{[(NH_3)_3Cu]_2O_2\}^{2+}$ (**3**). Calculations on **3** show that this model is clearly inadequate even for qualitative energetic modeling of dioxygen binding while it is successful in describing spectral, structural, and magnetic properties. Calculations show that the isomerization of **3** is endoergic by 49 kJ/mol, and there is essentially no energy barrier relative to the higher energy $(\mu\text{-}O)_2$ isomer. The dioxygen binding energy of **3** is endoergic by 160 kJ/mol as opposed to the exoergic binding in both **1** and **2**.

Introduction

Tolman and co-workers recently reported the synthesis of N-substituted derivatives of $\{[LCu]_2O_2\}^{2+}$, L = 1,4,7-triazacyclononane[1] (**1**), which reversibly bind dioxygen and reversibly break the O−O bond through the isomerization of their $Cu_2(\mu\text{-}\eta^2\text{:}\eta^2\text{-}O_2)$ (**A**), and $Cu_2(\mu\text{-}O)_2$ (**B**) core isomers.[2] The interconversion of these isomers is the first experimental evidence for a general mechanism suggested for biological activation and evolution of dioxygen.[3]

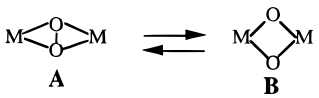

Dinuclear iron, manganese, and copper active sites with core structures **A** and **B** are common in enzymes which are responsible for O−O bond activation or evolution. A tetranuclear manganese cluster which consists of two $Mn_2(\mu\text{-}O)_2$ units (structure **B**) is the active site of photosystem II and responsible for dioxygen evolution from water. The reverse reaction, the cleavage of the dioxygen O−O bond, occurs at dinuclear iron and copper sites of several enzymes with core structure **A**. Oxyhemocyanin and oxytyrosinase are copper enzymes containing core structure **A** in their active sites. The former is a reversibly binding oxygen carrier[4a] in arthropods and mollusks while the latter enzyme functions as monooxygenase and carries out the oxidation of phenols.[4b]

N-Substituted derivatives of **1** in isomer **A** are inorganic mimics of the active site of oxyhemocyanins[5] which also contain a $Cu_2(\mu\text{-}\eta^2\text{:}\eta^2\text{-}O_2)$ core structure. The two d^9 copper centers are antiferromagnetically coupled through a superexchange mechanism[6] which is responsible for the diamagnetic, EPR silent, singlet ground state. The O−O stretching frequency is significantly reduced to 725−760 cm^{-1} from the dioxygen frequency and is close to a typical peroxide stretching frequency. These complexes have two characteristic absorption bands at 350 nm (ϵ = 20 000 M^{-1} cm^{-1}) and 550 nm (ϵ = 1000 M^{-1} cm^{-1}) and a feature in the circular dichroism spectrum at 480 nm ($\Delta\epsilon$ = +2.5 M^{-1} cm^{-1}) with no corresponding feature in the absorption spectrum. The Cu−Cu, O−O, and Cu−O distances are 3.6, 1.41, and 1.9 Å, respectively.

[⊗] Abstract published in *Advance ACS Abstracts,* September 15, 1997.

(1) (a) Mahapatra, S. Halfen, J. A.; Wilkinson, E. C.; Pan, G.; Cramer, C. J.; Que, L., Jr.; Tolman, W. B. *J. Am. Chem. Soc.* **1995**, *116*, 9785. (b) Mahapatra, S.; Halfen, J. A.; Wilkinson, E. C.; Pan, G.; Cramer, C. J.; Que, L., Jr.; Tolman, W. B. *J. Am. Chem. Soc.* **1995**, *117*, 8865−8866.

(2) (a) Proserpio, D. M.; Hoffman, R.; Dismukes, G. C. *J. Am. Chem. Soc.* **1992**, *114*, 4374. (b) Feig, A. L.; Lippard, S. J. *Chem. Rev.* **1994**, *94*, 759. (c) Pecoraro, V. L.; Baldwin, M. J.; Gelasco, A. *Chem. Rev.* **1994**, *94*, 807.

(3) Halfen, J. A.; Mahapatra, S.; Wilkinson, E. C.; Kaderli, S.; Young, V. G., Jr.; Que, L., Jr.; Zuberbühler, A. D.; Tolman, W. B. *Science* **1996**, *271*, 1397.

(4) (a) Lontie, R.; Vanquickenborne, L. In *Metal Ions in Biological Systems*; Siegel, H., Ed.; Dekker: New York, 1974; Vol. 3, pp 183−200. (b) Mason, H. S. *Nature* **1956**, *177*, 79−81.

(5) (a) Magnus, K.; Ton-That, H.; Carpenter, J. E. In *Bioinorganic Chemistry of Copper*, Karlin, K. D., Tyeklar, Z., Eds.; Chapman and Hall: New York, 1993; pp 143−150. (b) Magnus, K.; Ton-That, H.; Carpenter, J. E. *Proteins: Struct., Funct., Genet*. **1994**, *19*, 302. (c) Volbeda, A.; Hol, G. J. *J. Mol. Biol.* **1989**, *209*, 249.

(6) (a) Anderson, P. W. *Solid State Phys.* **1963**, *14*, 99. (b) Hay, P. J.; Thiebault, J. C.; Hoffman, R. *J. Am. Chem. Soc.* **1975**, *97*, 4884. (c) Yamaguchi, K.; Takahara, Y.; Fueno, T.; Nasu, K. *Jpn. J. Appl. Phys.* **1987**, *26*, L2307. (d) De Loth, P.; Cassoux, P.; Daudey, J.-P. *J. Am. Chem. Soc.* **1981**, *103*, 4007. (e) Gerloch, M. A local view in magnetochemistry. In *Progress in Inorganic Chemistry*; Lippard, S., Ed.; Interscience Publications: New York, 1979.

S0020-1669(97)00396-0 CCC: $14.00 Published 1997 by the American Chemical Society

The $Cu_2(\mu\text{-}O)_2$ complexes have strikingly different properties compared to those of their $\mu\text{-}\eta^2\text{:}\eta^2$ analogues. Their UV−vis features are at 324 nm (ϵ = 11 000 M^{-1} cm^{-1}), 440 nm (ϵ = 13 000 M^{-1} cm^{-1}), and the O−O stretching resonance Raman band is at 600 cm^{-1}. The Cu−Cu, Cu−O, and O−O distances are 2.794, 1.81, and 2.287 Å, respectively.[2]

One intriguing aspect of the discovery of the fast core isomerization of **1** is that other dinuclear copper complexes with core structure **A** have similar structural, magnetic, and spectroscopic properties but show different chemistry. Of particular interest are the N-substituted derivatives of $\{[LCu]_2O_2\}^{2+}$, L = hydrotris(pyrazolyl)borate (**2**), synthesised by Kitajima et al., which were the first structurally characterized inorganic mimics of the active site of oxyhemocyanin.[7] While **1** binds dioxygen reversibly and undergoes reversible core isomerization, **2** binds dioxygen irreversibly and exhibits only isomer **A**. This paper aims to explain the similarities of structural, spectroscopic, and magnetic properties and the differences in the chemical behavior of **1** and **2**. Previous theoretical studies related to **1** and **2** and the oxyhemocyanin active site were based on a model system, $\{[(NH_3)_3Cu]_2O_2\}^{2+}$ (**3**). Although calculations on **3** are sufficient to describe qualitatively the bonding of **1** and **2**, they cannot explain the differences between the chemistry of these systems.

Our calculations are based on density functional theory (DFT) at the generalized gradient approximation (GGA) level (see Computational Details). Gradient-corrected DFT has proved to be a successful tool in modeling energetics, structures, and spectroscopy of transition metal systems.[8]

Bernardi and co-workers recently reported calculations on **3** (in isomer **A**) and smaller models by complete active space self-consistent field (CASSCF), by complete active space perturbation theory (CASPT2), and by DFT methods.[9] Another recent paper by Bernardi et al. investigates the binding process of triplet oxygen to hemocyanin.[10]

Solomon and co-workers carried out an investigation of the electronic structure and electronic spectrum of oxy-Hc and other copper enzymes based on combined experimental spectroscopic and theoretical self-consistent field scattered-wave X_α (SCF-X_α-SW) calculations.[11,12] Eisenstein, Getlicherman, and their co-workers have applied extended Hückel theory (EHT)[13] to a model system with two copper cations ligated by six imidazole rings and bridged by a peroxide.

Cramer and co-workers carried out calculations on **3** by minimum basis set restricted Hartree−Fock (HF) calculation and by the broken symmetry X_α method and single-point calculations at the CASPT2 level.[14,1b] Most recently, Cramer et al. reported calculations on **3** by minimal basis set HF geometry optimization followed by CASPT2 single-point calculations serving to describe the potential surface of isomerization of **1**.[14b]

Computational Details

The reported calculations were carried out with the Amsterdam density functional (ADF) program system version 2.0.1 derived from the work of Baerends et al.[15] and developed at the Free University of Amsterdam[16] and at the University of Calgary.[17] All optimized geometries calculated in this study are based on the local density approximation[18] (LDA) augmented with gradient corrections to the exchange[18b] and correlation[18c] potentials. These optimizations were carried out by the direct inversion of iterative subspace for geometry (GDIIS) technique[19] with natural internal coordinates.[20] We have combined the ADF program with the GDIIS program[21] and previously implemented the skeletal internal coordinates.[22] The internal coordinates were generated by the INTC program[23] and augmented by hand.

The atomic orbitals on copper were described by an uncontracted triple-ζ STO basis set,[24] while a double-ζ STO basis set was used for carbon, nitrogen, oxygen, and hydrogen; a single-ζ polarization function was used on all atoms. The $1s^2$ configuration on carbon, nitrogen, and oxygen and the $1s^22s^22p^6$ configuration of copper were assigned to the core and treated by the frozen-core approximation.[15] A set of auxiliary s, p, d, f, g, and h STO functions, centered on all nuclei, was used in order to fit the molecular density and represent the Coulomb and exchange potentials accurately in each SCF cycle.[25]

The numerical integration accuracy parameter which approximately represents the number of significant digits for the scalar matrix elements was gradually increased to 4.5 until convergence with respect to integration accuracy was reached. This numerical accuracy is sufficient to determine energies within a fraction of a kilojoule/mole, and bond distances within 0.001 Å (which is more accurate than predicted by the numerical integration accuracy parameter). It is important to emphasize the scalable numerical accuracy implemented in the ADF program, which makes it possible to significantly reduce the computational cost at the initial stages of geometry optimization, when the gradient is still large. These calculations could be carried out on single processor workstations due to efficient algorithms implemented in the

(7) (a) Kitajima, N.; Koda, T.; Hashimoto, S.; Kitagawa, T.; Moro-oka, Y. *J. Chem. Soc., Chem. Commun*. **1988**, 151−152. (b) Kitajima, N.; Fujisawa, K.; Moro-oka, Y.; Toriumi, K. *J. Am. Chem. Soc.* **1989**, *111*, 8975−8976.
(8) Ziegler, T. *Chem. Rev.* **1991**, *91*, 651.
(9) Bernardi, F.; Bottoni, A.; Casadio, R.; Fariselli, P.; Rigo, A. *Int. J. Quantum Chem.* **1996**, *58*, 109−119.
(10) Bernardi, F.; Bottoni, A.; Casadio, R.; Fariselli, P.; Rigo, A. *Inorg. Chem.* **1996**, *35*, 5207−5212.
(11) (a) Ross, P. K.; Solomon, E. I. *J. Am. Chem. Soc.* **1990**, *112*, 5871−5872. (b) Ross, P. K.; Solomon, E. I. *J. Am. Chem. Soc.* **1991**, *113*, 3246−3259. (c) Tuczek, F.; Solomon, E. I. *J. Am. Chem. Soc.* **1994**, *116*, 6916−6924.
(12) Slater, J. C. *The Self-Consistent Field for Molecules and Solids*; McGraw-Hill: New York, 1974; Vol. 4.
(13) (a) Eisenstein, O.; Giessner-Prettre, C.; Maddaluno, J.; Stussi, D.; Weber, J. *Arch. Biochem. Biophys*. **1992**, *296*, 247−255. (b) Getlicherman, H.; Giessner-Prettre, C.; Maddaluno, J. *J. Phys. Chem.* **1996**, *100*, 6819−6824.
(14) (a) Mahapatra, S.; Halfen, J. A.; Wilkinson, E. C.; Pan, G.; Wang, X.; Young, V. G., Jr.; Cramer, C. J.; Que, L., Jr.; Tolman, W. B. *J. Am. Chem. Soc.* **1996**, *118*, 11555. (b) Cramer, C. J.; Smith, B. A.; Tolman, W. B. *J. Am. Chem. Soc.* **1996**, *118*, 11283. (c) Smith, B. A.; Cramer, C. J. *J. Am. Chem. Soc.* **1996**, *118*, 5490.
(15) Baerends, E. J.; Ellis, D. E.; Ros, P. *Chem. Phys.* **1973**, *2*, 41.
(16) (a) Ravenek, W. In *Algorithms and Applications on Vector and Parallel Computers*; te Riele, H. J. J., Dekker, Th. J., van de Vorst, H. A., Eds.; Elsevier: Amsterdam, 1987. (b) Boerrigter, P. M.; te Velde, G.; Baerends, E. J. *Int. J. Quantum Chem.* **1988**, *33*, 87. (c) te Velde, G.; Baerends, E. J. *J. Comput.Phys.* **1992**, *99*, 84.
(17) (a) Fan, L.; Ziegler, T. *J. Chem. Phys.* **1991**, *94*, 6057. (b) Fan, L.; Ziegler, T. *J. Chem. Phys.* **1991**, *95*, 7401. (c) Fan, L.; Versluis, L.; Ziegler, T.; Baerends, E. J.; Ravenek, W. *Int. J. Quantum Chem.* **1988**, *S22*, 173. (d) Fan, L.; Ziegler, T. *J. Chem. Phys*. **1992**, *96*, 9005. (e) Fan, L.; Ziegler, T. *J. Phys. Chem.* **1992**, *96*, 6937.
(18) (a) Vosko, S. H.; Wilk, L.; Nusair, M. *Can. J. Phys.* **1980**, *58*, 1200. (b) Becke, A. D. *Phys. Rev. A* **1988**, *38*, 2398. (c) Perdew, J. P. *Phys. Rev. B* **1986**, *33*, 8822; **1986**, *B34*, 7046.
(19) (a) Császár, P.; Pulay, P. J. *J. Mol. Struct.*, **1984**, *114*, 31. (b) Pulay, P. *Chem. Phys. Lett.* **1980**, *73*, 393. (c) Pulay, P. *J. Comput. Chem.* **1982**, *3*, 556.
(20) (a) Fogarasi, G.; Zhou, X.; Taylor, P. W.; Pulay, P. *J. Am. Chem. Soc.*, **1992**, *114*, 8191. (b) Pulay, P.; Fogarasi, G.; Pang, F.; Boggs, J. E. *J. Am. Chem. Soc.* **1979**, *101*, 2550.
(21) Programmed by A. G. Csaszar and P. G. Szalay, Eötvös University, Budapest, Hungary, 1984.
(22) (a) Bérces, A. *J. Comput. Chem.* **1997**, *18*, 45−55. (b) Bérces, A.; Ziegler, T. *J. Phys. Chem.* **1994**, *98*, 13233. (c) Bérces, A.; Ziegler, T.; Fan, L. *J. Phys. Chem.* **1994**, *98*, 1584.
(23) INTC program to generate natural internal coordinates, P. Pulay and G. Fogarasi, 1992, Univerity of Arkansas, Fayetteville.
(24) (a) Snijders, G. J.; Baerends, E. J.; Vernooijs, P. *At. Data Nucl. Data Tables* **1982**, *26*, 483. (b) Vernooijs, P.; Snijders, G. J.; Baerends, E. J. Slater Type Basis Functions for the whole Periodic System. internal report; Free University of Amsterdam, The Netherlands, 1981.
(25) Krijn, J.; Baerends, E. J. Fit functions in the HFS-method. internal report (in Dutch); Free University of Amsterdam: The Netherlands, 1984.

ADF program and custom modifications of the geometry optimization. We also emphasize the importance of full geometry optimization without any constraint on Cu−Cu or Cu−N or O−O distances; such constraints were used even in the most recent works.

Although our approach represents improvements over previous theoretical models for oxy-Hc and its mimics, we still do not take into account some effects such as N-substituents, finite temperature, solvation, zero-point energy corrections, and basis set superposition error. Most of the error should be related to these neglected effects and not to error in the DFT energies. Gradient-corrected DFT calculations were repeatedly shown to provide exceptionally good energetics for transition metal systems.[8] We expect that isomerization energies should be reliable within a few kilojoules/mole, but addition or dissociation energies, where the neglected effects are more important, could be off by 10−20 kJ/mol compared to experimental values.

Results and Discussion

Magnetic Coupling. All oxy-Hc mimics contain two antiferromagnetically coupled d^9 copper centers. In the theoretical description of such interactions by single determinant wave function the broken-symmetry solution has to be considered.[26] Solomon et al. studied the electronic structure and electron transition energies of side-on and end-on bonded dioxygen complexed to copper monomer and dimer complexes by broken-symmetry SCF-X_α-SW calculations. The calculations on **3** by Solomon et al. converged to a broken-symmetry solution, and the CASSCF calculations of Bernardi et al. also resulted in a significant contribution from the ionic configuration in the ground state wave function. On the other hand, in the series of dicopper peroxo complexes considered by Solomon et al. this system had the most delocalized electron spin density, indicating the most strongly coupled system. Further, Bernardi et al. also have shown that the CASSCF method resulted in a qualitatively incorrect structure with almost broken O−O bond of 1.80 Å (experimental 1.4). In the light of these contradicting theoretical findings, the question arises if it is necessary to describe the electronic structure of these systems within the broken-symmetry formalism. We found that broken-symmetry gradient-corrected density functional calculations converged to the symmetrical, fully delocalized solution on all model systems. Our results indicate that the ground state of oxyhemocyanin mimics can be well described by a restricted single-determinant molecular orbital model with the Becke Perdew gradient-corrected functional. It is important to emphasize here that other density functionals, especially with a mixed Hartree−Fock exchange term, may yield a broken-symmetry wave function for the same systems. The qualitative description of the molecular orbitals in our study is very similar to previous descriptions based on a broken-symmetry wave function. Detailed discussion of the theoretical aspects is given elsewhere.[27]

The Geometry of the Core Structure. The highest symmetry of all systems is C_{2h}; however, the C_{2h} conformation of **1** corresponds to an eclipsed arrangement about the C_5-C_6 bond. The more stable staggered arrangement reduces the symmetry to C_2 or C_i (Figure 1). Calculated total energies of **1** optimized with imposed C_{2h}, C_2, C_i, or C_1 point group symmetry are within 2kJ/mol of one another, the C_i conformer being the most stable. Calculations with no symmetry restriction also converged to the C_i geometry. In spite of the close energetics, the core geometries are quite different for the C_{2h}, C_2, and C_i symmetry conformers due to the weak Cu−O bonds. The facile distortion of the core into an asymmetrical structure in the C_i symmetry

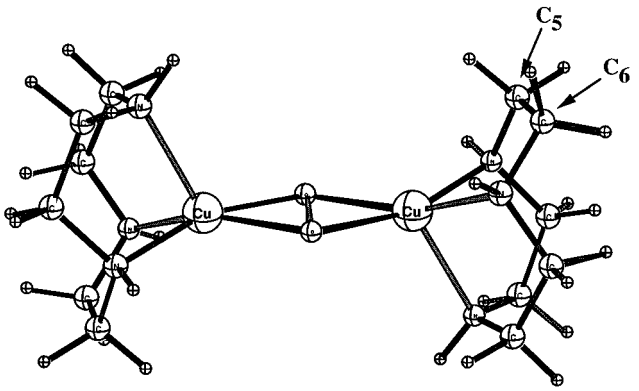

Figure 1. The preferred conformation of **1**.

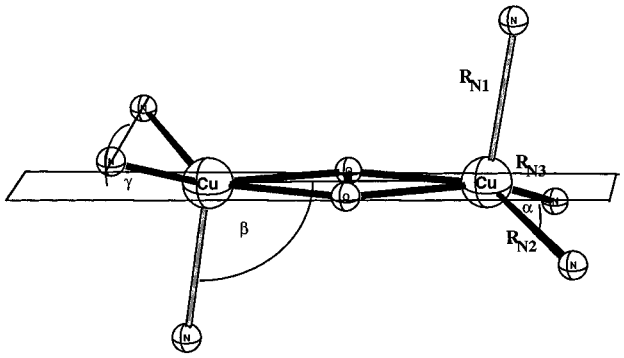

Figure 2. Important structural parameters of the Cu_2O_2 core.

Table 1. The Geometrical Parameters of the μ-η^2:η^2-O_2 $Cu_2O_2N_6$ Core Structure[a]

		1			
μ-η^2:η^2-O_2	exptl[b]	C_{2h}	C_i	**2**	**3**
R_{CuCu}	3.6	3.706	3.716	3.700	3.815
R_{OO}	1.41	1.467	1.468	1.458	1.440
R_{CuO1}	1.90	1.993	1.966	1.988	2.040
R_{CuO2}	1.92	1.993	2.029	1.988	2.040
R_{CuN1}	2.26	2.208	2.190	2.252	2.247
R_{CuN2}	2.00	2.078	2.043	2.014	2.089
R_{CuN3}	2.00	2.078	2.143	2.014	2.089
α	92.7	82.1	81.8	92.5	105.1
β	114	118.3	120.1	113.0	99.2
γ	17	21.0	23.5	20.7	33.2
O−Cu−Cu−N_1	90.0	90.0	85.2	90.0	90.0

[a] Distances in angstroms, angles in degrees. [b] Reference 3 and references therein.

conformers of **1** suggests a possible transformation between μ-η^2:η^2-O_2 and *trans*-μ-1,2-O_2 isomers. Further distortion from the C_{2h} to the C_i coordinate results in a *trans*-μ-1,2-O_2 dinuclear complex.[28] Such interconversion was previously suggested to take place in oxy-Hcs by Ling et al. on the basis of resonance Raman spectroscopy and normal coordinate analysis.[29]

The important geometrical parameters of **1**, **2**, and **3** are defined on Figure 2, and the calculated structural data of the μ-η^2:η^2-O_2 and $(\mu$-$O)_2$ isomers and the transition state of the isomerization are listed in Tables 1, 2, and 3, respectively. The calculated geometrical parameters are in agreement with the experimental data within the expected accuracy of the models. The calculated Cu−Cu and O−O distances are somewhat too long compared to experiment, and the Cu−Cu distances are

(26) (a) Mouesca, J.-M.; Chen, J. L.; Noodleman, L.; Bashford, D.; Case, D. A. *J. Am. Chem. Soc*. **1994**, *116*, 11898−11914. (b) Noodleman, L.; Case, D. A. *Adv. Inorg. Chem.* **1992**, *38*, 423−470. (c) Noodleman, L.; Baerends, E. J. *J. Am. Chem. Soc.* **1984**, *106*, 2316−2327.
(27) Berces, A. Submitted to *Int. J. Quantum Chem. Symp*.
(28) Jacobson, R. R.; Tyeklar, Z.; Farooq, A.; Karlin, K. D.; Liu, S.; Zubieta, J. *J. Am. Chem. Soc.* **1988**, *110*, 3690−3692.
(29) Ling, J.; Nestor, L. P.; Czernuszewicz, R. S.; Spiro, T. G.; Frackiewicz, R.; Sharma, K. D.; Loehr, T. M.; Sanders-Loehr, J. *J. Am. Chem. Soc.* **1994**, *116*, 7682−91.

Table 2. The Geometrical Parameters of the (μ-O)$_2$ $Cu_2O_2N_6$ Core Structure[a]

		1			
μ-O_2	exptl[b]	C_{2h}	C_i	**2**	**3**
R_{CuCu}	2.79	2.748	2.746	2.819	2.810
R_{OO}	2.29	2.451	2.456	2.348	2.371
R_{CuO1}	1.81	1.841	1.849	1.834	1.838
R_{CuO2}	1.80	1.841	1.835	1.834	1.838
R_{CuN1}	2.30	2.302	2.292	2.450	2.431
R_{CuN2}	1.99	2.022	2.056	1.978	2.032
R_{CuN3}	1.99	2.022	2.003	1.978	2.032
α		82.0	81.9	90.4	97.9
β		117.5	117.6	115.3	100.8
γ		17.3	17.8	14.7	15.0
O−Cu−Cu−N_1		90.0	85.3	90.0	90.0

[a] Distances in angstroms, angles in degrees. [b] Reference 3 and references therein.

Table 3. The Geometrical Parameters of the Transition State of Core Isomerization[a]

	1		
	C_{2h}	C_i	**2**
R_{CuCu}	3.261	3.258	3.240
R_{OO}	1.861	1.886	1.839
R_{CuO1}	1.877	1.873	1.863
R_{CuO2}	1.877	1.891	1.863
R_{CuN1}	2.263	2.247	2.326
R_{CuN2}	2.066	2.041	2.024
R_{CuN3}	2.066	2.102	2.024
α	81.5	81.4	90.3
β	119.8	118.0	112.1
γ	20.3	19.4	15.8
O−Cu−Cu−N_1	90.0	83.9	90.0

[a] Distances in angstroms, angles in degrees.

sensitive to ligand substitution. Comparing the structures of **1**, **2**, and **3**, the most striking differences are in the N−Cu−N bond angles, which is a consequence of the different constraints set by the ligands. The nine-membered-ring ligand of **1** is the most constraining with small N−Cu−N bond angles, while the ammonia ligands of **3** maximize the N−Cu−N bond angles within the square pyramidal configuration. To illustrate the change in the ligand conformations upon oxygen binding and cleavage, we show the CuL fragment of the monomeric Cu^IL, isomers **A** and **B** of all systems in Figure 3. The α and γ angles (cf. Figure 2 and Tables 1 and 2) differ by 7° and 18° between the two core isomers of **3**, while the corresponding differences are insignificant for **1** and **2**. The theoretical model system **3** correctly predicts the existence of both core isomers and the Cu−Cu, Cu−O, O−O, and Cu−N distances, but lacks the rigidity of ligands compared to the synthetic systems.

To establish the mechanism of the core isomerization and to find the activation barrier of the reaction, it is important to locate the transition state which we found for the isomerization of **1** and **2**. The transition states of **1** and **2** are close to the average of the structural parameters of the two isomers. On the other hand, linear transit calculations on **3** between 2.9 and 3.4 Å Cu−Cu separation yield transit point energies between the energies of isomers **A** and **B**. Furthermore, these findings indicate that **3** does not have any transition state for core isomerization which is comparable to that of **1** or **2**. The lack of the similarity for the transition state in spite of the similarity in the stable structures is explained in the next section by considering the different contributions to the total energy.

To calculate the dioxygen binding energies it was essential to determine the geometry of the monomer Cu^IL; the corresponding data are shown in Table 4. The oxygenated forms of all systems have one pair of long apical Cu−N bonds and two pairs of shorter axial Cu−N bonds. In the monomer corresponding to **1** and **2**, the situation is reversed; there are one short and two long Cu−N bonds. The monomer of **3**, $\{Cu(NH_3)_3\}^+$, has a slightly distorted 3-fold symmetric structure. The angular arrangements of the ammonia ligands in **3** are different from the those of **1** and **2**, which introduces problems in energetic modeling, as we shall discuss in the next sections.

Energetics of O_2 Binding and Isomerization. To compare the energetics of dioxygen binding in **1**, **2**, and **3** we calculated the reaction internal energy (ΔE) corresponding to

$$2Cu^IL + O_2 \rightarrow Cu_2O_2L_2 \qquad (1)$$

The theoretical ΔE values can be regarded as an approximation to the observable ΔH reaction enthalpies. In spite of the structural similarities, the energies of the oxygenation reaction in which **1**, **2**, and **3** are formed are significantly different. The oxygenation reaction yielding **3** is substantially endoergic, $\Delta E = 160$ kJ/mol, while the reactions of **1** and **2** are both exoergic, namely, $\Delta E = -60$ and -184 kJ/mol, respectively. The ΔE values of **1** and **2** are both in accord with the experimental observation that O_2 binding of **1** is reversible while that of **2** is irreversible. The observed dioxygen binding enthalpy of the structurally similar reversibly binding dicopper complex [L = xylene-bridged bis(2-pyridyl)ethylamine (XYL)] equals -62 ± 1 kJ/mol.[30] The observed oxygenation enthalpies of other dinuclear copper complexes with tetradentate tris(2-pyridyl)-ethylamine (TMPA) and related ligands, which also bind dioxygen reversibly, are between -50 and -80 kJ/mol.[31] Our calculated $\Delta E = -60$ kJ/mol for **1** is well within the experimental range of systems that reversibly bind dioxygen.

The calculated energies of core isomerization from the $Cu_2(\mu\text{-}\eta^2\text{:}\eta^2\text{-}O_2)$ to the $Cu_2(\mu\text{-}O)_2$ isomers of **1**, **2**, and **3** are 1, 12, and 49 kJ/mol, respectively. The barrier heights relative to the $Cu_2(\mu\text{-}\eta^2\text{:}\eta^2\text{-}O_2)$ form of **1** and **2** are 33 and 37 kJ/mol while there is no barrier associated with the isomerization of **3** in excess of 49 kJ/mol isomerization energy. Both the negligible isomerization energy and the low barrier of **1** are in line with the observed fast interconversion of the core isomers. Experimental results suggest that the core isomerization is faster than the rate-determining step of mononuclear adduct formation, which has a measured activation enthalpy of 37 kJ/mol.

The reversible and irreversible nature of oxygen binding of **1** and **2**, respectively, is in line with the different binding energies. In spite of the large differences in binding energies, the core isomerization energy profiles of **1** and **2** are similar except for the slightly endoergic nature of the isomerization of **2**. The 12 kJ/mol isomerization energy of **2**, however, does not explain why the (μ-O)$_2$ core isomer was not observed. Considering that $[Cu[HB(3,5\text{-}Me_2pz)_3]]_2(O_2)$ was suggested to decompose into a putative μ-oxo dinuclear copper(II) complex $[Cu[HB(3,5\text{-}Me_2pz)_3]]_2O$,[32] it is likely that the necessary dioxygen cleavage step of this decomposition process takes place through core isomerization from **A** to **B**. This explanation is consistent not only with the previously suggested mechanism of decomposition[32] but also with the increased thermal stability of **2** upon N-substitution by bulky ligands which can prevent core isomerization. Although **1** is less thermally stable than **2**, **1** decomposes through a different mechanism. Therefore, **1** can be observed in both core isomers while **2** can only be found in isomer **A**.

(30) Cruse, R. W.; Kaderli, S.; Karlin, K. D.; Zuberbüler, A. D. *J. Am. Chem. Soc.* **1988**, *110*, 6882−6883.
(31) Karlin, K. D.; Wei, N.; Jung, B.; Kaderli, S.; Niklaus, P.; Zuberbüler, A. *J. Am. Chem. Soc.* **1993**, *115*, 9506−9514.
(32) Kitajima, N.; Moro-oka, Y. *Chem. Rev.* **1994**, *94*, 737−757.

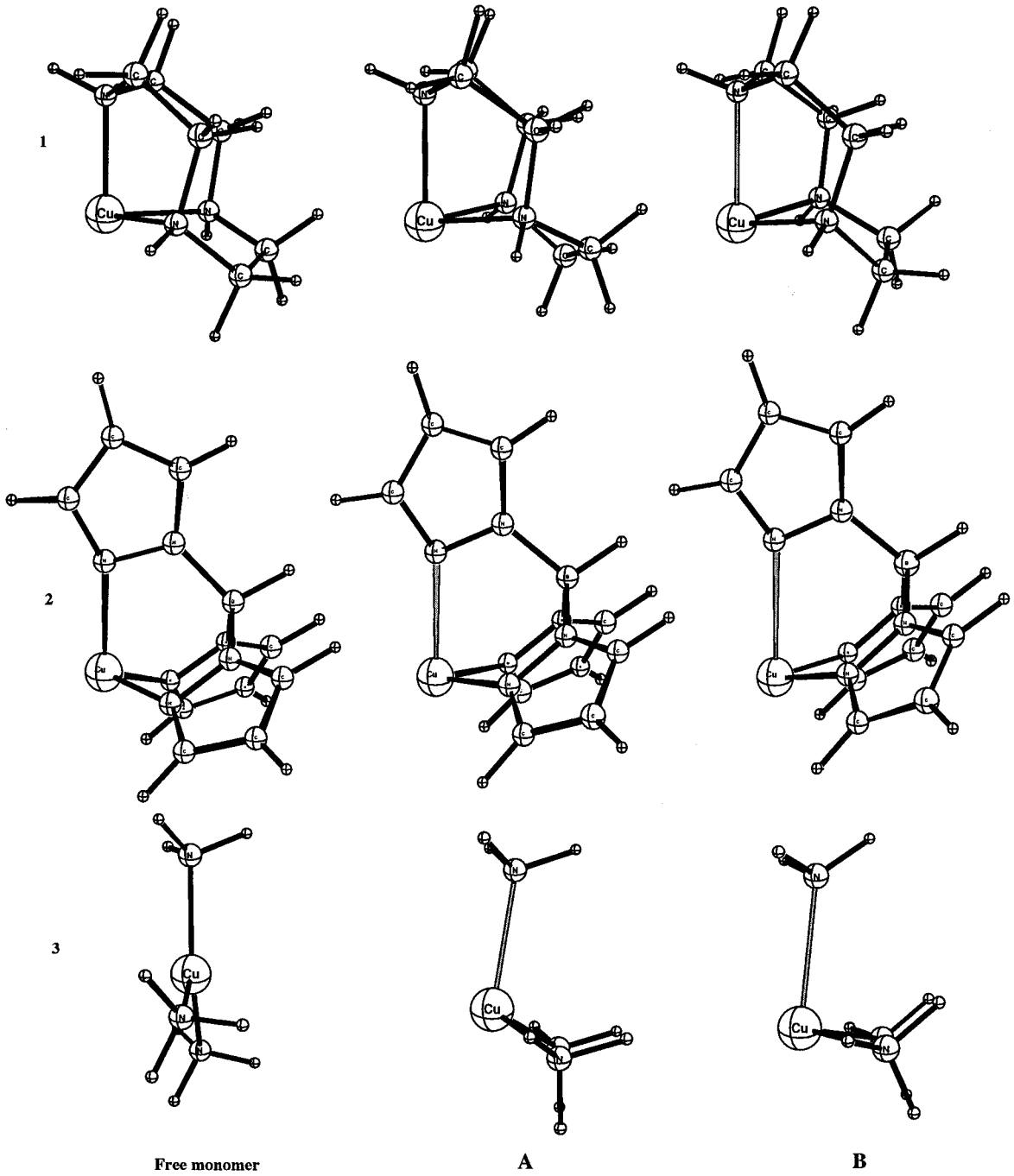

Figure 3. The conformations of ligands in monomeric $Cu^{I}L$ and dinuclear isomers **A** and **B**.

Table 4. The Geometrical Parameters of the Mononuclear $Cu^{I}L$ Complexes[a]

	1			
	C_{2h}	C_i	**2**	**3**
R_{CuN1}	2.068	2.059	2.018	2.092
R_{CuN2}	2.096	2.092	2.025	2.092
R_{CuN3}	2.096	2.126	2.025	2.092
α	85.2	84.8	99.0	119.9
β	90.4	89.9	100.0	119.9
γ	90.4	90.8	100.0	120.2

[a] Distances in angstroms, angles in degrees. Numbering of N atoms: 1 is apical; 2 and 3 are equatorial atoms. α, β, and γ are N_i-Cu-N_j bending angles with $i,j = (2,3)$, (1,2), and (1,3), respectively.

Energy Decomposition. More insight into the bonding can be gained through a bond analysis developed by Ziegler and Rauk[33] based on a breakdown of the binding energy into different components. This approach has been successfully applied to other bridged dinuclear metal complexes by Jacobsen et al.[34] Although this procedure is quite mathematical, the aim is to explain bonding in three simple terms: orbital interaction energies (ΔE_{el}), steric interaction ($\Delta E°$), and preparation energy (ΔE_{prep}) as shown in eq 2. The total binding energy ($\Delta E_{binding}$)

$$\Delta E_{binding} = \Delta E_{el} + \Delta E° + \Delta E_{prep} \qquad (2)$$

in our calculations represents the reaction energy of dioxygen addition to two $Cu^{I}L$ fragments; the corresponding results are summarized in Table 5. The term ΔE_{el} represents the main

(33) (a) Ziegler, T.; Rauk, A. *Theor. Chim. Acta* **1977**, *46*, 1. (b) Ziegler, T. A General Energy Decomposition Scheme for the Study of Metal-Ligand Interactions in Complexes, Clusters and Solids. *NATO ASI*, in press. (c) Ziegler, T.; Rauk, A. *Inorg. Chem.* **1979**, *18*, 1558. (d) Ziegler, T.; Rauk, A. *Inorg. Chem.* **1979**, *18*, 1755.
(34) Jacobsen, H.; Kraatz, H.-B.; Ziegler, T.; Boorman, M. P. *J. Am. Chem. Soc.* **1992**, *114*, 7851−7860.

Table 5. Binding Energies of O_2 Binding and Binding Energy Decomposition (kJ/mol)

	1			
	C_{2h}	C_i	**2**	**3**
μ-η^2:η^2-O_2: Isomer **A**				
binding[a]	−60	−60	−184	163
ligand preparation	17	17	51	118
electronic contributions				
B_g (π*)	−592		−572	−489
A_u (σ*)	−18		−18	−10
steric interactions				
Pauli repulsion	812		870	816
Coulomb electrostatic	−291		−511	−268
μ-O_2: Isomer **B**				
binding[a]	−59	−59	−172	214
ligand preparation	60	60	117	225
electronic contributions				
B_g (π*)	−832		−823	−826
A_u (σ*)	−769		−700	−704
steric interactions				
Pauli repulsion	1778		1783	1825
Coulomb electrostatic	−800		−1019	−798
Transition State				
activation energy[b]	33	33	37	

[a] ΔE corresponding to $2Cu^{I}L + O_2 \rightarrow L_2Cu_2O_2$. Only the terms discussed in the text are listed. The O_2 preparation energies are 100 kJ/mol for isomer **A** and 640 kJ/mol for isomer **B**, on average. The electronic contributions from the A_g and B_u irreducible representations are negligible. [b] Relative to isomer **A**.

features of the common theory by Parr and Pearson in which the binding energy is related to the differences in electronegativity and hardness between interacting fragments.[35] The electronic contributions in our system arise from the donation of copper d electrons into the π* and σ* orbitals. The π* and σ* contributions to binding energy can be individually calculated since these two interactions correspond to different irreducible representations under C_{2h} symmetry (A_u and B_g, respectively). The steric interaction term arises from the competing attractive Coulomb electrostatic and the dominating repulsive Pauli interactions. The preparation energy reflects on the rigidity of the ligands, and this energy is required for the deformation of the separate fragments from their initial equilibrium position to the conformation in the final complex.

Comparison of the binding energy components of **1** and **2** (cf. Table 5) shows that most terms are very similar; particularly, both the π* and σ* orbital interaction energies are close in **1** and **2**. The minor differences in the ligand preparation and the σ* term of the $(\mu\text{-}O)_2$ isomer do not explain the differences in the binding energy. On the other hand, the electrostatic (Coulomb) components offsetting the steric repulsion of **1** and **2** are −291 and −511 kJ/mol for isomer **A** and −800 and −1019 kJ/mol for isomer **B**, respectively. We conclude that this difference is responsible for the stronger dioxygen binding of **2**. *The similarity in the electronic contributions explains the similar structural, magnetic, and spectroscopic properties of* ***1*** *and* ***2*** *while the difference in the Coulomb energy term explains their different chemical behavior.*

It is interesting to find out why the theoretical system **3** fails to predict even qualitatively the binding energy and isomerization energy and why the isomerization potential does not show a barrier. The binding energy of **3** is 220 and 273 kJ/mol more endoergic than that of **1** in isomers **A** and **B**, respectively. The π* interaction energy of **3** in isomer **A** is about 100 kJ/mol different from that of **1** and **2**, which accounts for a good portion of the difference. However, the most crucial difference between **1** and **3** is in the preparation energy. The nine-membered-ring ligand of **1** is already constrained in the monomer and requires only 17 kJ/mol for deformation into the final position in isomer **A**. On the other hand, the floppy ammonia ligands of **3** are substantially reorganized upon oxygen binding, which requires an increased preparation energy of 118 kJ/mol for isomer **A**. The same effect is responsible for the endoergic isomerization of **3**; the preparation energy corresponding to core structure **B** of **3** is 225 kJ/mol as opposed to 60 and 117 kJ/mol for **1** and **2**. Since the ligand conformational energetics dominates the isomerization of **3**, this explains why **3** isomerizes in a barrierless transition, in contrast to **1** and **2**.

In spite of the global disagreement between **1** and **3**, there are some remarkable similarities in the steric repulsion terms. The Coulomb energy components of **1** and **3** with neutral ligands are nearly the same but distinctly different from the corresponding component of **2** with negatively charged ligands. The differences between the Coulomb terms of ligands with different charges are expected. However, these data suggest that the negative charge of the hydrotris(pyrazolyl)borate stabilizes **2** and is responsible for the stronger binding without any significant change in the orbital interactions. This finding implies that *complexes with ligands of similar donor and acceptor properties but with different total charge can have different chemical reactivity.*

Comparison with Previous Theoretical Studies. While most structural, magnetic, and spectroscopic properties are determined by local interactions at the Cu_2O_2 core, the chemistry is determined by the total energies of the systems, to which the ligands make significant contributions. As the present results show, ligands have to be included explicitly in the model for realistic energetic studies. The calculations on **1** and **2** could explain both the differences and the similarities in their observed properties, which was not possible on the basis of **3**. Previous theoretical studies of **1** and **2** and the oxyhemocyanin active site were based on model systems like **3**. While **3** is successful in predicting the existence of both core isomers and in describing the electronic transitions, core vibrational frequencies, and magnetic properties which are related to the Cu_2O_2 chromophore, this model is incapable of predicting the total energies of binding and core isomerization correctly. Cramer et al. described the isomerization potential surface of **1** as flat on the basis of STO3G-HF geometry optimization and CASPT2 single-point energy calculations on **3**.[14b] The aim of Cramer et al.'s paper was only to describe the fundamental aspects of the surface and not to give a quantitative description. The present GGA calculations, which are more appropriate for transition metal systems, show that the isoergic isomers of **3** found by Cramer et al. are entirely fortuitous. Furthermore, the flat potential they describe would predict fluxional behavior which is inconsistent with the experimental data.

Our analysis indicates that the ligand conformation energy plays an important role in fine-tuning the energetic balance so that models which ignore these effects cannot describe the total reaction energetics correctly. *Similarly, theoretical models of enzymes which neglect the protein backbone are inappropriate for studying the reactivity of the active site.*

Recent work by Bernardi et al. uses an even simpler model, $\{[(NH_3)_2Cu]_2O_2\}^{2+}$, to describe the energetics of dioxygen binding in hemocyanin.[10] Their calculated binding energy is highly exoergic, namely, $\Delta E = -52$ kcal/mol (−218 kJ/mol), which is inconsistent with the reversible nature of dioxygen binding in hemocyanin. Bernardi et al. neglect the apical ligand of the oxyhemocyanin active site on the basis that these are

(35) (a) Pearson, R. G. *Inorg. Chem.* **1988**, *27*, 734. (b) Parr, R. E. Pearson, R. G. *J. Am. Chem. Soc.* **1983**, *105*, 7512.

longer and weaker Cu−N bonds compared to the equatorial bonds. However, the apical Cu−N bond distance in hemocyanin is only 2.0 Å, which increases to 2.6 Å only upon oxygenation. This large reorganization indicates a significant change in the ligand−metal interaction and shows the importance of the apical ligand in the binding mechanism. Further, comparison with the binding energy of **3** shows that the inclusion of the apical ligand reverses the sign of the binding energy in this simple model.

Electronic Structure, Electronic Transition Energies, and Magnetic Properties. While the chemical properties of **1** and **2** are clearly different, their electronic and vibrational spectra and their magnetic properties are similar. To test whether the calculations can reproduce the similarities in these properties we studied the charge transfer transition energies, magnetic coupling constants, and charge population of both conformers of **1**, **2**, and **3**. Since the results were in essential agreement with what was intuitively expected, we only summarize the most important points here.

Comparing the molecular orbitals of **1**, **2**, and **3**, the theoretical system **3** gives a good qualitative representation of the electronic structure of the inorganic mimics. The differences between different systems are related to the extent of ligand participation. The predicted electron transition energies are also very close. For example, the π^*_v transitions of **1** and **3** are calculated to be 36 000 and 37 500 cm^{-1}, respectively. The magnetic interaction constant (−2J) which equals the singlet−triplet splitting, was found to be proportional to the HOMO−LUMO gap; the $-2J$ constants for the **A** isomer of **1** and **3** are 6163 and 3800 cm^{-1}, respectively. Ligand participation in the LUMO orbital is responsible for the difference.

It is also of interest to compare partial charges on copper and oxygen between **1** and **2**, especially since **2** has charged ligands and this charge is suggested to be responsible for the stabilization of the complex. The calculated partial charges on the Cu and O atoms of the complexes are very similar in both systems, which is consistent with the similarities in the orbital interactions. Our charge analysis also allows the direct calculation of the amount of charge transferred from one fragment to the other. On average, the total charge transferred from two mononuclear $Cu^{I}L$ complexes to the dioxygen is −0.65 and −1.02 for the μ-η^2:η^2-O_2 and the $(\mu\text{-}O)_2$ isomer, respectively, which indicates a high degree of covalency in both isomers.

Conclusions

We studied the energetics of oxygen binding in two inorganic mimics and a theoretical model of the oxyhemocyanin active site. The calculated binding energies were in line with the observed reversible binding of **1** and irreversible binding in **2**. Binding energy decomposition made it possible to interpret the differences; Coulomb stabilization due to the negative charge on the $HB(pz)_3$ ligand is suggested to be responsible for the stronger binding in **2**. On the other hand, orbital interaction energies of **1** and **2** are essentially the same, which explains their similar structural, magnetic, and spectroscopic properties. We also described the transition state of the core isomerization of **1** and **2** and showed the existence of a small barrier in line with experimental results. According to these results, core isomerization of **2** is not observed simply because isomerization leads to decomposition of the complex.

The theoretical system **3** with ammonia ligands, while successful for the interpretation of bonding and spectra, is inappropriate for the prediction of reactivity. Bond energy decomposition showed that the lack of restraints on the ligands made the ligand conformation energy to be the dominating factor in the total reaction energy and led to excessive ligand reorganization. For this reason, **3** isomerizes without a barrier and exhibits endoergic dioxygen binding and isomerization energies. Although models like **3** are common in theoretical energetic modeling, they should be used only if the associated energy changes are significantly larger than the neglected ligand effects.

Acknowledgment. I thank Professor Peter Pulay for providing the INTC program which generates the input for natural coordinate optimization. I gratefully acknowledge a visiting fellowship from the National Research Council Canada. I also thank my colleagues at the Steacie Institute for discussions; I am especially grateful to Drs. Heinz-Bernhard Kraatz and Allen East for discussions of the chemistry of these systems and for comments on the manuscript. Further, I thank Drs. Keith Ingold and Willem Siebrand for carefully reading the manuscript and for their valuable suggestions. The initial calculations were done by Shelly Pinder (University of Lethbridge). This paper is issued as NRCC No. 39133.

IC970396O